

## Measurements from ground and balloons during APE-GAIA – A polar ozone library

H.K. Roscoe<sup>a,\*</sup>, S.R. Colwell<sup>a</sup>, J.D. Shanklin<sup>a</sup>, J.A. Karhu<sup>b</sup>, P. Taalas<sup>b</sup>, M. Gil<sup>c</sup>,  
M. Yela<sup>c</sup>, S. Rodriguez<sup>c</sup>, C. Rafanelli<sup>d</sup>, H. Cazeneuve<sup>e</sup>, C.A. Villanueva<sup>f</sup>,  
M. Ginsburg<sup>f</sup>, S.B. Diaz<sup>g</sup>, R.L. de Zafra<sup>h</sup>, G. Muscari<sup>h</sup>, G. Redaelli<sup>i</sup>, R. Dragani<sup>i</sup>

<sup>a</sup> British Antarctic Survey/NERC, Madingley Road, Cambridge CB3 0ET, UK

<sup>b</sup> FMI, Finland

<sup>c</sup> INTA, Madrid, Spain

<sup>d</sup> CNR-IFA, Italy

<sup>e</sup> Direccion Nacional del Antartico, Cerrito 1248, 1010 Buenos Aires, Argentina

<sup>f</sup> Servicio Meteorologico Nacional, 25 de Mayo 658, Buenos Aires, Argentina

<sup>g</sup> CADIC Ushuaia, Argentina

<sup>h</sup> SUNY-Stoneybrook, USA

<sup>i</sup> University of L'Aquila, L'Aquila, Italy

Received 9 August 2004; received in revised form 28 February 2005; accepted 2 March 2005

### Abstract

Many long-term monitoring sites in Antarctic regions, which deploy ground-based stratospheric remote sensors and fly radiosondes or ozonesondes on balloons, supported the Airborne Polar Experiment in September and October 1999. Support consisted of supplying data to the campaign in real time, and in some cases by increasing the frequency of measurements during the campaign. The results will strengthen scientific conclusions from the airborne measurements. But results from these sites are allowing important scientific studies of new aspects of the ozone hole in their own right, because like the aircraft and its campaign, many sites traverse the vortex edge and are close to the largest source of lee waves, or measure infrequently observed trace gases such as HNO<sub>3</sub>. Examples of such studies are the behaviour and value of NO<sub>2</sub> in midwinter, ozone filamentation with no apparent horizontal advection, the frequency and amplitude of gravity waves over the Antarctic Peninsula, mixing in the lowest stratosphere in Antarctic spring, the mechanism and frequency of HNO<sub>3</sub> enhancement above the ozone peak in midwinter, and trends in UV dose in southern South America.

© 2005 COSPAR. Published by Elsevier Ltd. All rights reserved.

**Keywords:** Antarctic; Ozone; Remote sensors; Trace gases; Ground-based

### 1. Introduction

Since its discovery by Farman et al. (1985), many aspects of the Antarctic ozone hole have become well understood. Despite the provisions of the Montreal

Protocol, the current ozone depletion is as bad as ever (Fig. 2 – see Fig. 1 for a map of sites). Indeed, there is speculation that recovery of the Antarctic ozone hole may be delayed by interactions with increased greenhouse gases (e.g., Shindell et al., 1998; Roscoe and Lee, 2001).

A new picture of the ozone hole emerged with the discovery that a broad edge region of the vortex,

\* Corresponding author. Tel.: +441223221431.

E-mail address: [h.roscoe@bas.ac.uk](mailto:h.roscoe@bas.ac.uk) (H.K. Roscoe).

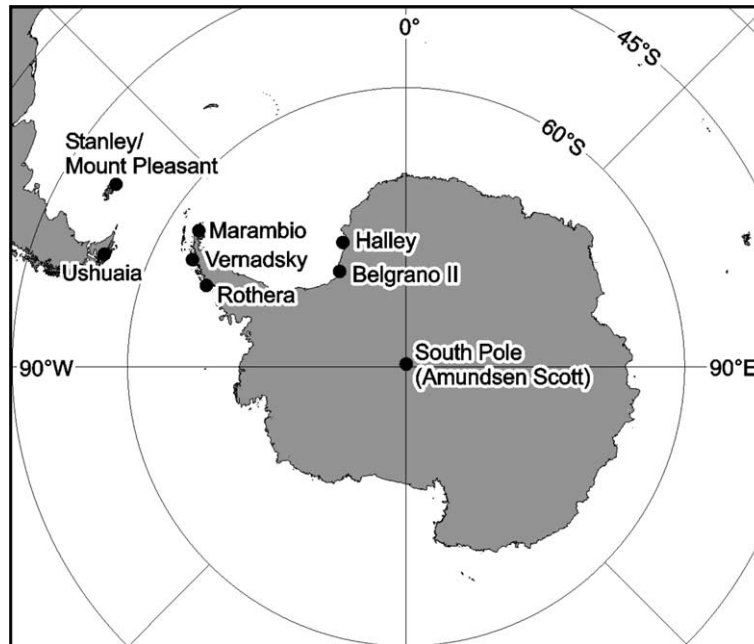


Fig. 1. Map of Antarctic regions, showing locations of the monitoring stations used for the measurements described in this work. Amundsen-Scott is the designated name of the station at the South Pole. Mount Pleasant Airport, 20 km from Stanley, is relevant to Section 3.5. Vernadsky is the station that used to be called Faraday.

comprising about half the area of the vortex, is isolated from the vortex core until after chlorine activation has ceased (Lee et al., 2001). The behaviour of the ozone loss in 1999 is shown in Fig. 3, which includes plots of the mean total ozone above a pair of sites in the edge region and a pair in the core. The root-mean-square (rms) difference in ozone between the sites in the vortex core was only 10 Dobson Units (DU) despite their being over  $2^\circ$  latitude apart, illustrating the significant degree of mixing in the core. By contrast, the rms difference in ozone at the sites in the edge region was over 16 DU despite their being only  $1.1^\circ$  latitude apart, illustrating the poorer mixing within the edge region, as predicted by Lee et al. (2001).

For these and other new or poorly understood aspects of ozone-hole science, the Airborne Polar Experiment-Geophysica Aircraft In Antarctica (APE-GAIA) campaign was undertaken by international investigators (Carli et al., 2000). The aircraft was equipped with remote and in situ sensors, and undertook five flights from Ushuaia in southern Argentina between 16 September and 15 October 1999.

In Antarctica, there are many long-term monitoring sites which deploy ground-based stratospheric remote sensors or have routine flights of radiosondes or ozonesondes on balloons, and which are located close to the planned campaign flights. Some sites measure infrequently observed trace gases in common with the aircraft. Investigators with apparatus at these sites agreed to support the APE-GAIA campaign by

supplying preliminary values of their measurements to the campaign headquarters in real time, to help with forecasts of special events to be covered by individual flights (lee waves, filamentation). At some sites, extra radiosondes were flown, which were important to improve the quality of meteorological forecasts used to plan the flights. These supporting measurements are being used to add value to airborne measurements.

But such medium and long-term measurement series can address important new issues of ozone-hole science in their own right. Our data set helps address new issues by being from sites that traverse the vortex edge region and are close to the largest source of lee waves, or by measuring infrequently observed trace gases such as  $\text{HNO}_3$ . In this paper, we air several such issues, describe progress in their study, and discuss preliminary conclusions. We also provide tables of the various instrument types and measurement dates so that others might seek to make use of this important data set for further studies.

## 2. Measurements

The measurements made during the APE-GAIA campaign are listed in Table 1, which includes references for methodology and sources of error of some non-commercial instruments. Fig. 1 shows a map of the sites, and the breadth and scope of the measurements are

Table 1  
Ground-based and balloon-borne measurements in support of APE-GAIA from 15 September 1999 to 16 October 1999

Site	Latitude (°S)	PI	Instrument	Measurement
Ushuaia	54.8	Rafanelli	Brewer	Total O <sub>3</sub> & NO <sub>2</sub> , O <sub>3</sub> profiles, UVB irradiance
		Cazeneuve	Dobson	Total O <sub>3</sub>
		Diaz	Spectroradiometer <sup>a</sup>	Irradiance 280–620 nm, erythemat UV irradiance
		Yela	UV-vis <sup>b</sup>	Total O <sub>3</sub> & NO <sub>2</sub>
Marambio	64.2	Villanueva	Dobson	Total O <sub>3</sub>
		Yela	UV-vis <sup>b</sup>	Total O <sub>3</sub> & NO <sub>2</sub>
		Taalas	Sondes (14)	Profiles of O <sub>3</sub> & T
		Taalas	Sondes (43)	Profiles of T
Vernadsky	65.3	Shanklin	Dobson	Total O <sub>3</sub>
Rothera	67.6	Roscoe	UV-vis <sup>b</sup>	Total O <sub>3</sub> & NO <sub>2</sub>
		Colwell	Sondes (12)	Profiles of T
Halley	75.6	Shanklin	Dobson	Total O <sub>3</sub>
		Colwell	Sondes (30)	Profiles of T
Belgrano	77.9	Cazeneuve	Brewer	Total O <sub>3</sub> & NO <sub>2</sub> , O <sub>3</sub> profiles, UVB irradiance
		Yela	Sondes (6)	Profiles of O <sub>3</sub> & T
		Yela	UV-vis <sup>b</sup>	Total O <sub>3</sub> & NO <sub>2</sub>
S Pole	90.0	De Zafra	Microwave <sup>c</sup>	Profiles of HNO <sub>3</sub>

<sup>a</sup> Irradiances at Ushuaia are measured by a scanning double monochromator (Biospherical Instruments SUV-100) with resolution 1 nm and wavelength accuracy 0.01 nm, as part of the NSF UV Monitoring Program.

<sup>b</sup> The UV-vis spectrometer at Rothera is a SAOZ-512, those from Yela are of INTA design (Gil and Cacho, 1992); for details of spectral analysis procedures, other instruments and intercomparisons see Roscoe et al. (1999).

<sup>c</sup> Deconvolution of pressure-broadened rotational line spectra near 269.2 GHz; for estimates of accuracy and vertical resolution see De Zafra et al. (1997).

illustrated in Figs. 2–8. Measurements are available from <http://apegaia.iroec.fir.cnr.it/> “Staff only”, “Auxiliary Measurements”. Many of the instruments or sonde

deployments were parts of long-term programmes, listed in Table 2, where measurements are available from the investigators.

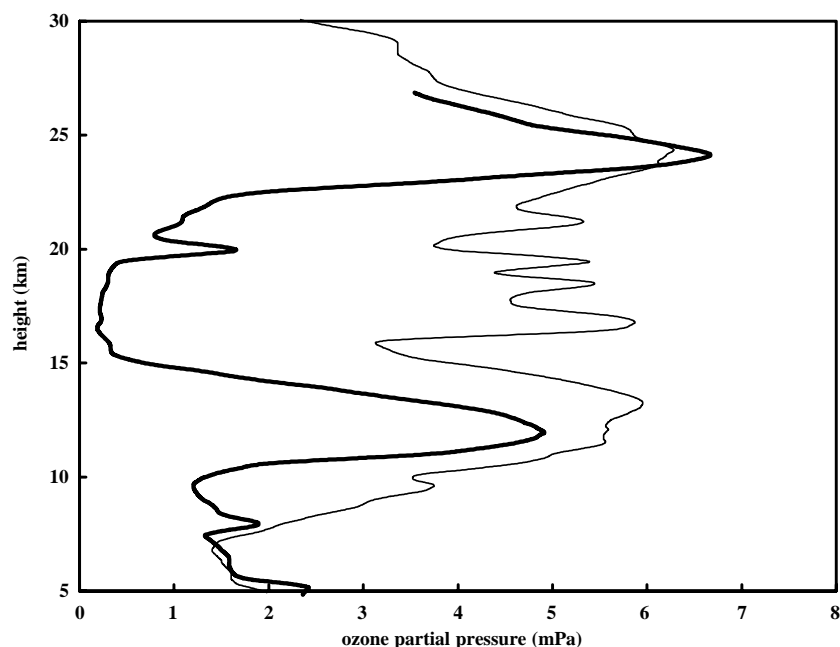


Fig. 2. Ozone profile measured from Belgrano (77.9°S), on 2 October 1999 (thicker line) when the ozone hole is fully developed, and on 14 September 1999 (thinner line). In October there is almost no ozone between 15 and 20 km, illustrating the absence of any signs of recovery in the ozone hole. Even in September there is significant ozone loss since the return of sunlight to the core of the vortex here in August – the ozone maximum exceeded 15 mPa at nearby Halley during early August in 1987. These measurements have been smoothed by about 0.2 km, for clarity.

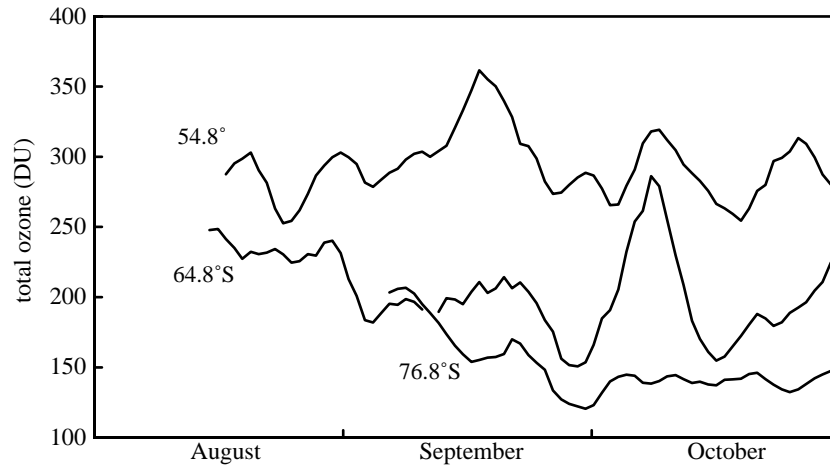


Fig. 3. Total ozone in southern South America, in Antarctica in what is often the edge region of the stratospheric vortex, and in the vortex core. Measurements are from Ushuaia (54.8°S), the mean of Marambio (64.2°S) and Vernadsky (65.3°S, formerly Faraday), and the mean of Halley (75.6°S) and Belgrano (77.9°S). Values were smoothed with 5-day running means, in order to guide the eye. Note that ozone-poor air from the edge region reaches southern South America for two periods in late September and in October, when the Sun is high enough at noon to cause UV damage to the population.

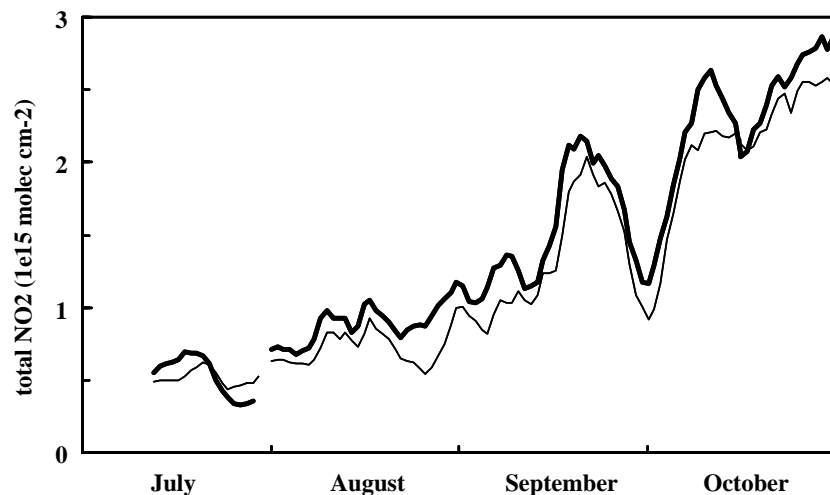


Fig. 4. Total vertical column of  $\text{NO}_2$  measured at morning twilight (thinner line) and evening twilight (thicker line) by the INTA/DNA UV–vis zenith-sky spectrometer at Marambio (64.2°S), smoothed by a 5-day running mean. As discussed in Section 3.1, these measurements show rather more  $\text{NO}_2$  near midwinter than in the early 1990s at Faraday, only 1.1° further south.

### 3. Discussion

#### 3.1. $\text{NO}_2$ in midwinter

As shown in Fig. 4, the  $\text{NO}_2$  amount in July at Marambio (64.2°S) is about  $0.5 \times 10^{15}$  molecule  $\text{cm}^{-2}$ . This is a typical pattern at Marambio – indeed the midwinter average from 1994 to 2000 (not shown) is about  $0.7 \times 10^{15}$  molecule  $\text{cm}^{-2}$ . By contrast, midwinter  $\text{NO}_2$  amounts measured by a similar ground-based zenith sky spectrometer in the early 1990s at Faraday, 1.1° further south, were only about  $0.2 \times 10^{15}$  molecule  $\text{cm}^{-2}$  (Roscoe et al., 2000).

Very small amounts of total  $\text{NO}_2$  in Antarctic winter mean that significant removal of  $\text{NO}_x$  (denoxification) must almost certainly have taken place. The converse is not necessarily true because there could be zero  $\text{NO}_2$  due to denoxification at some altitudes but not at others. However, the observed difference of near-zero  $\text{NO}_2$  at one location and rather more  $\text{NO}_2$  nearby must suggest a strong gradient in denoxification, at least at some altitudes. This might be expected given the weak mixing within the edge region of the vortex here. However, POAM II measurements of  $\text{NO}_2$  in midwinter show very weak gradients between Faraday and Rothera (C. Randall, private communication).

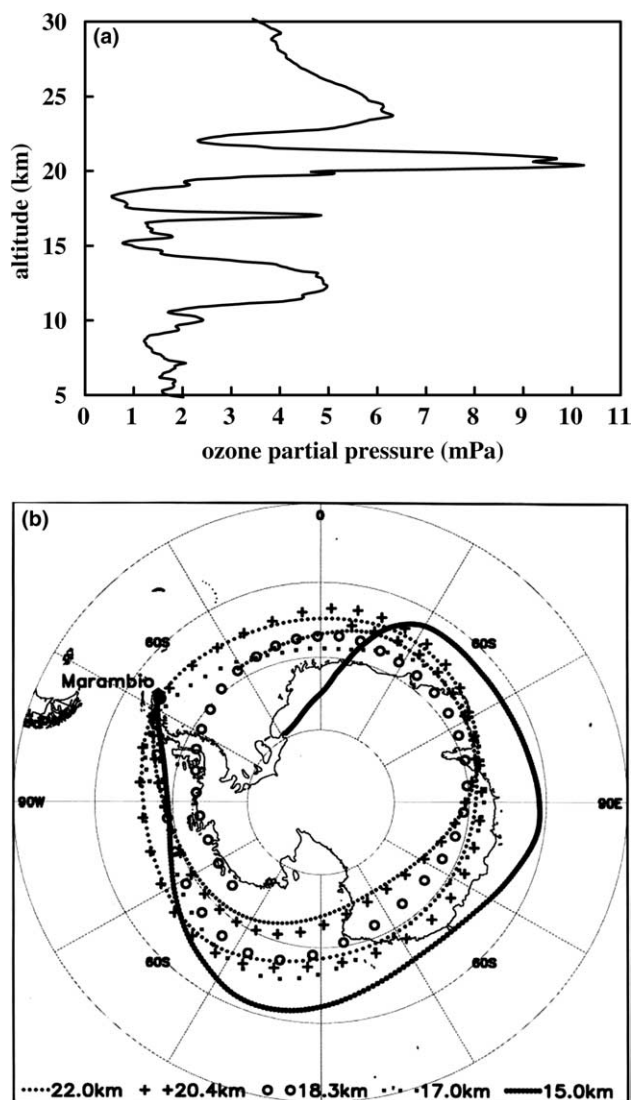


Fig. 5. (a) Ozone profile at Marambio on 29 September 1999 showing major ozone loss at some altitudes and much less ozone loss at others. (b) 7-day domain-filling back trajectories at each layer of the ozone profile at Marambio on 29 September 1999. This illustrates a contradiction concerning the layer at 20.4 km, discussed in Section 3.2.

An alternative explanation might lie in the different analysis procedures. Analysis at Marambio uses the conventional assumption that the effective amount in the reference spectrum is the actual amount on the day it was measured. Analysis at Faraday determines the amount of  $\text{NO}_2$  in the reference spectrum by means of chemically modified Langley plots, and a test with the conventional determination produced larger  $\text{NO}_2$  values. This would suggest that the gradient is an artefact of the differences in analysis styles between Faraday and Marambio, except that  $\text{NO}_2$  amounts at Belgrano just after sunrise were  $<0.1 \times 10^{15}$  molecule  $\text{cm}^{-2}$  (not shown) using a similar analysis style to Marambio.

Hence we now have disagreement between various data sets and analyses about the gradient in midwinter

$\text{NO}_2$  across the edge region of the vortex. This will hopefully be resolved in future work which may follow on from the EU project “QUILT” (Arlander et al., 1999), by including chemically modified Langley-plot analysis of measurements from Marambio as well as Rothera, and model predictions of the expected latitudinal gradients of  $\text{NO}_2$  in Antarctica.

### 3.2. Ozone filamentation

Ozone profiles above Marambio showed layered structures in 10 of the 14 soundings during the campaign. Fig. 5(a) shows one of the more extreme cases. At the time of this sounding, the vortex edge was north of Marambio, so that most of the sampled air was either from the vortex core or its edge region. Domain filling trajectories (DFTs) were calculated backwards for 7 days. The trajectories in Fig. 5(b) show that ozone minima originate from well inside the vortex.

Table 3 lists the PV values at the start of these trajectories (the DFT-PV values). Their ratios to PV values calculated on the day of the sounding at the vortex edge suggest that only one (17.0 km) of the two ozone maxima originates from closer to the vortex edge than the ozone minima. The back trajectory of the layer of the ozone maximum at 20.4 km has a striking similarity to that at 22.0 km in Fig. 5(b), which suggests that the maximum at 20.4 km cannot be explained by isentropic advection.

### 3.3. Wave event of 2 October

In Fig. 6(a), the low-temperature minimum on 2 October at 13.1 km and maximum at 15.4 km (just before losing contact with the sonde in the strong vortex winds) are obvious. The altitude difference between the first minimum and first maximum is 2.3 km, similar to the values of 2 and 3 km observed and calculated at two locations in a mountain lee wave over Scandinavia by Wirth et al. (1999). During the APE-GAIA flight of 2 October, airborne lidars observed a PSC centred at 12.5 km and an optically thicker one at 19.5 km (Cairo et al., 2000). This is a vertical wavelength of 7 km, in between the 5.5 and 6.5 km observed and calculated by Wirth et al. (1999), and the 10 km calculated for a lee wave by Carslaw et al. (1998).

The difference between the temperatures at the first minimum and first maximum is 13.6 K. This is larger than the 7 K observed and calculated by Wirth et al., but similar to the 15 K they found between the first maximum and second minimum. It is similar to the amplitude of 16–22 K deduced from ER2 observations near Rothera by Bacmeister et al. (1990), despite partial blocking of the lee wave which greatly reduced its amplitude.

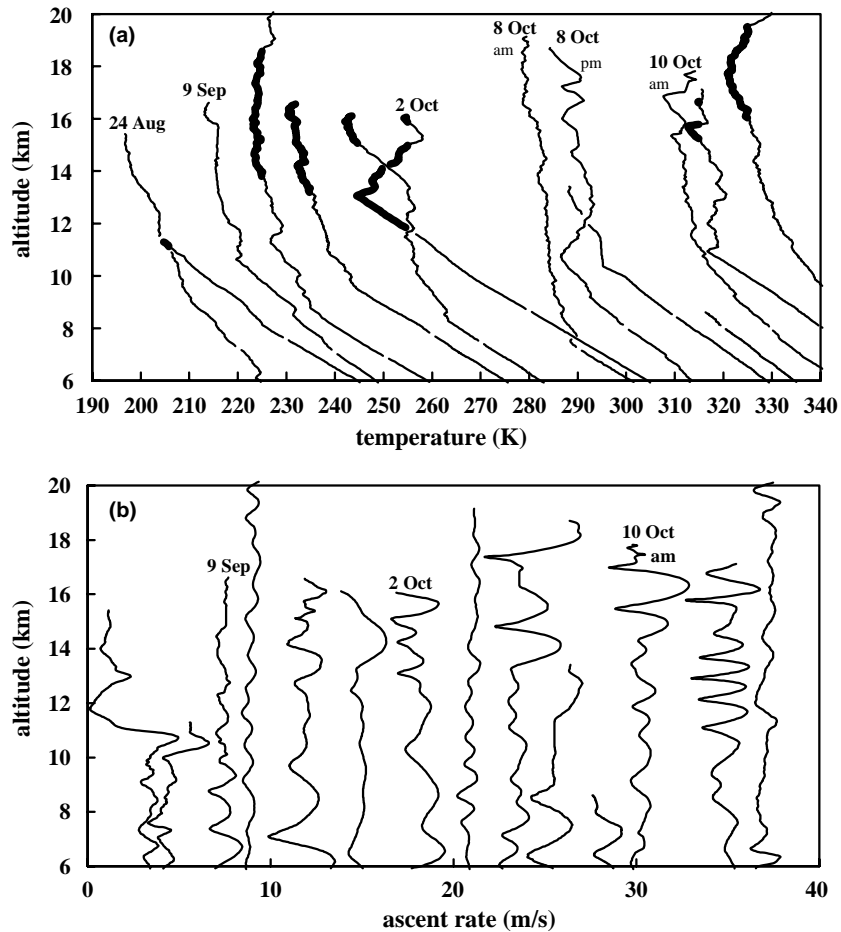


Fig. 6. Radiosonde data from Rothera ( $67.6^{\circ}\text{S}$ ), showing (top) temperature and (below) ascent rates. Dates from left to right are 24 Aug, 2, 9, 18, 21 & 23 Sep, 2 Oct, 8 Oct am & pm, 9 Oct am & pm, 10 Oct am & pm, 12 Oct. Each temperature is offset from the previous curve by 10 K; the temperature scale applies to the left-hand curve; 220 K is indicated by a short gap in each curve; temperatures below 195 K are in bold, illustrating the large minimum on 2 Oct at 13 km discussed in Section 3.3. Ascent rates are offset by hand by arbitrary amounts for clarity, and are smoothed by about 300 m. The ascent rates have pronounced structure, with vertical wavelengths less than 3 km, as discussed in Section 3.4.

Hence it is tempting to ascribe this event entirely to a lee-wave over the Antarctic peninsula. However, the warmer temperatures in the upper troposphere on 2 October, together with PV and TOMS maps, suggest a major Rossby contribution to the wave event (Ferretti et al., 2000). In future work with mesoscale models, it will be important to establish the contributions to the wave type, not least because lee waves alone have too small a horizontal wavelength to be adequately resolved in current global meteorological analyses.

### 3.4. Frequency and amplitude of gravity waves over the Antarctic peninsula

Many wave structures with amplitudes of a few K or less can be seen in Fig. 6(a). Similar structures appear in the temperature profiles from Marambio in 1999 and in earlier years (not shown). In Fig. 6(b), the ubiquitous nature of these waves is clearer from the large variations in ascent rates, and the vertical wavelengths are seen to be

mostly between 1 and 2 km, typical of internal propagating gravity waves (e.g. Whiteway, 1999). Several examples of possible critical level filtering can be discerned in Fig. 6(b), which will be investigated in future work.

Although two of the profiles in Fig. 6(a) have wave amplitudes of 5 K peak-to-peak, most are less than 1 K. This is rather smaller than the mean amplitude in September and October in Antarctica given by Yoshiki and Sato (2000): about 2 K peak-to-peak. The amplitude of gravity waves at mid-latitudes is very important because their breaking in the stratosphere and mesosphere drives the circulation which brings HCl-rich air to the lower stratosphere in Antarctica and so allows ozone loss to occur. The role of gravity waves over Antarctica is less clear, but the momentum released in critical-level filtering at stratospheric altitudes can also provide a force to control convergence during descent. However, there are few radiosonde measurements near the Antarctic Peninsula. Hence future work will include analysis of the energy content of gravity waves in all the Rothera and Marambio

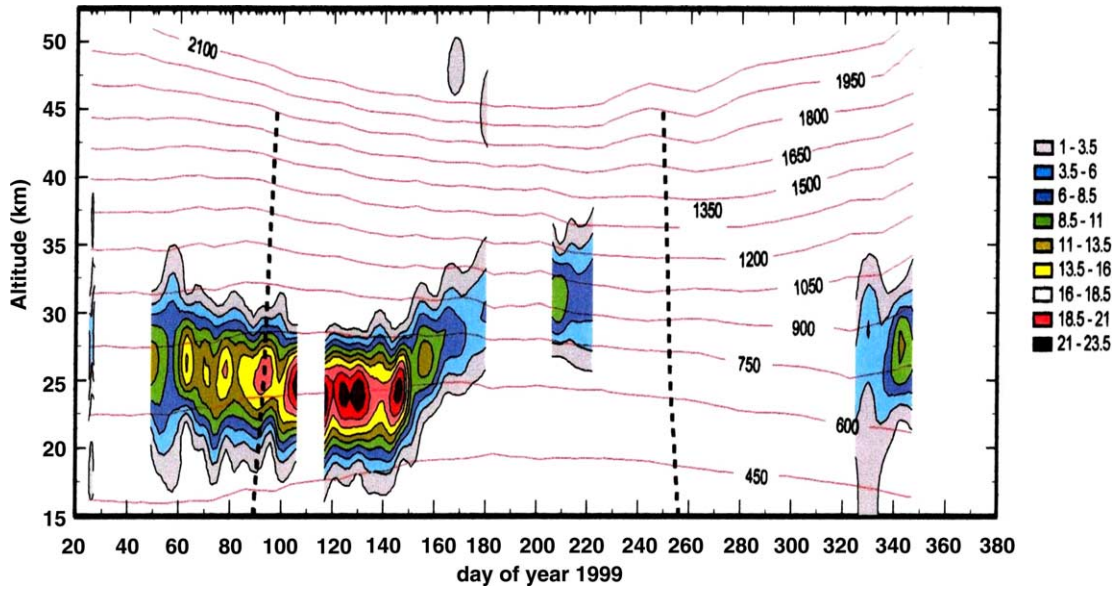


Fig. 7. Mixing ratio of  $\text{HNO}_3$  (ppbv) measured by the SUNY sub-millimetre sounder at South Pole (colour scale), and contours of potential temperature (K) from South Pole radiosondes supplemented by NCEP analyses above balloon limits (lines). The enhancement of  $\text{HNO}_3$  in the upper stratosphere beginning just before the break in data beginning on day 177 is similar to enhancements observed more completely when the sounder was deployed in 1993 and 1995, as discussed in Section 3.6.

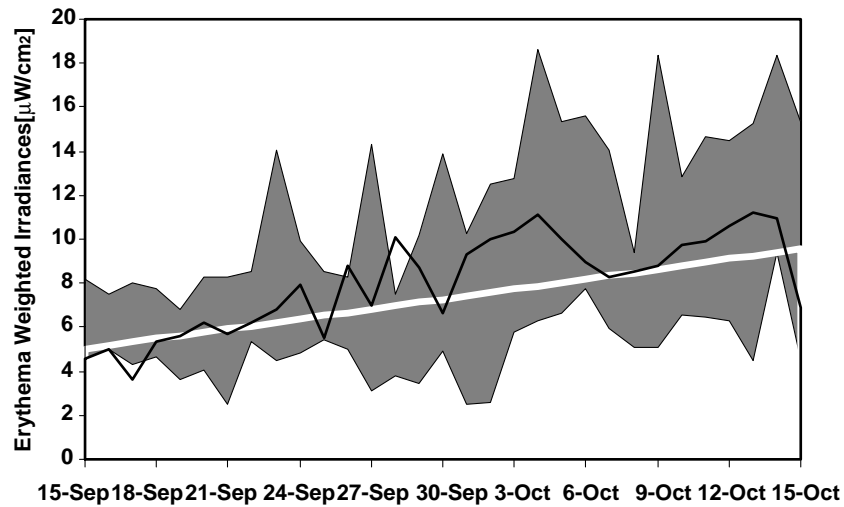


Fig. 8. Maximum daily values of erythemally weighted irradiance measured at Ushuaia in South America (54.8°S) from mid-September to mid-October in 1999 (black line) and from 1990 to 1998 (shaded area), together with calculated clear sky values (white line). The calculations use a cubic fit to daily ozone averaged from 1979 to 1982. The obvious increase from calculated values by the 1990s is discussed in Section 3.7.

data, independently in the troposphere and stratosphere so that low-altitude filtering can be determined.

High-resolution data such as that in Fig. 6 is not available prior to the modern Vaisalla receivers introduced in the 1980s. Worse, many meteorological archives only list temperatures at standard levels (100, 70 hPa, etc.) – too coarse to observe any but the longest-wavelength gravity waves. However, temperatures at critical levels (turning points) as well as standard levels, from radiosondes flown from Faraday from the 1950s to 1983, have recently been digitally archived. Hence attempts will also

be made to deduce energy content from this data set, and it will be examined for instances of possible Rossby reinforcement of lee waves of the kind discussed in Section 3.3, whose climatology is so important for formation of polar stratospheric clouds in this region of the ozone hole, and so for ozone loss.

### 3.5. Mixing in the lowest stratosphere in Antarctic spring

Below about 400 K in Antarctic winter and spring, widespread mixing is diagnosed from models forced

Table 2

Long duration ground-based and balloon-borne measurements from instruments in Table 1

Site	Dates	Instrument	Measurement	Frequency
Ushuaia	1988–now	Spectroradiometer	Irradiance 280–620 nm, erythema UV irradiance	1 h <sup>-1</sup> 1988–96, 4 h <sup>-1</sup> since
	1994–now	UV–vis	Total O <sub>3</sub> & NO <sub>2</sub>	Daily
	1994–now	Brewer	Total O <sub>3</sub> & NO <sub>2</sub> , O <sub>3</sub> profiles, UVB irradiance	Daily in 2–4 month/year, except 1998
	1995–now	Dobson	Total O <sub>3</sub>	Daily, but interruptions
Marambio	1994–now	UV–vis	Total O <sub>3</sub> & NO <sub>2</sub>	Daily
	1987–now	Dobson	Total O <sub>3</sub>	Daily <sup>a</sup>
	1988–now <sup>b</sup>	Sondes	Profiles of O <sub>3</sub> & T	2–8/month
	1982–now <sup>b</sup>	Sondes	Profiles of T	2/month to 1/day
Faraday/Vernadsky <sup>c</sup>	1957–now	Dobson	Total O <sub>3</sub>	Daily <sup>a</sup>
Rothera	1996–now	UV–vis	Total O <sub>3</sub> & NO <sub>2</sub>	Daily <sup>a</sup>
	2001–now	Sondes	Profiles of T	4–7/week
Halley	1956–now	Dobson	Total O <sub>3</sub>	Daily <sup>a</sup>
	1957–now	Sondes	Profiles of T	Daily
Belgrano	1995–now	UV–vis	Total O <sub>3</sub> & NO <sub>2</sub>	Daily <sup>a</sup>
	1999–now	Sondes	Profiles of O <sub>3</sub> & T	1–6/month
	1992–now	Brewer	Total O <sub>3</sub> & NO <sub>2</sub> , O <sub>3</sub> profiles, UVB irradiance	Daily <sup>a</sup>
South Pole <sup>d</sup>	1993, 95, 99	Microwave	Profiles of HNO <sub>3</sub>	1–2/week

<sup>a</sup> UV–vis spectrometers cannot measure if it is dark at noon; Dobsons and Brewers cannot measure if the solar elevation at noon is less than 10°.

<sup>b</sup> Sonde launches at Marambio were halted from 1985 to 1987, from April 1989 to June 1990, from March to April 1994, and from August to December 1997.

<sup>c</sup> The BAS site at Faraday was handed to the Ukrainian Antarctic Centre in 1996.

<sup>d</sup> The station at South Pole is formally designated as Amundsen-Scott.

Table 3

DFT-PV (see Section 3.2 for explanation) at altitudes of ozone maxima and minima above Marambio on 29 September 1999, and PV at the vortex edge (defined by the mean of the maximum gradients in gridded Southern Hemisphere PV for the 7 days of the trajectory)

Altitude (km)	Potential temperature (K)	Ozone maximum or minimum	PV of vortex edge (PV units)	DFT-PV (PV units)	DFT-PV/PV at edge
22.0	534	Minimum	–80	–125	1.56
18.3	443	Minimum	–28	–41	1.46
15.0	380	Minimum	–12	–18	1.50
20.4	501	Maximum	–56	–81	1.45
17.0	416	Maximum	–20	–25	1.26

by meteorological analyses (Lee et al., 2002), in contrast to the confinement of the vortex above. However, there are few radiosonde stations in Antarctica, particularly in any one longitude swath. Hence analyses must rely on satellite measurements, whose weighting functions are broad at the altitudes of the lower stratosphere in Antarctica (200 hPa), which therefore allows possible contamination from the upper troposphere. Because mixing is widespread in the upper troposphere, the diagnosed mixing in the lower stratosphere could be an artefact of the lack of radiosonde data.

This lack is worse between the centre and base of the Antarctic Peninsula because of the lack of a radiosonde station to monitor stratospheric temperatures since launches at Faraday ceased in 1983. But we now have a unique opportunity to test this possibility of artefacts in the analyses because of the extra

radiosondes launched from Marambio and Rothera during APE-GAIA. Marambio and Rothera link the operational sonde stations of South America and Mount Pleasant Airport to those of Halley and South Pole. With this in mind, the UK Met Office has made stratospheric analyses with and without the Marambio and Rothera data. Future work is planned to explore their differences in diagnosed mixing.

### 3.6. HNO<sub>3</sub> enhancement above ozone peak in midwinter

As well as the expected winter denitrification between about 15 and 25 km, the morphology of HNO<sub>3</sub> in Fig. 7 shows evidence of enhancement of HNO<sub>3</sub> at 45–50 km in midwinter (>1 ppbv at 46–51 km on days 161–165, >1 ppbv at 43–47 km on day 176). This midwinter enhancement is almost identical to that observed in win-

ter in 1993 and 1995 (McDonald et al., 2000) – 1993 and 1995 were the only other years of comprehensive submillimetre data at South Pole.

In Fig. 7, there is some evidence of the rapid descent of this enhancement to 32 km by day 225, although the missing data between days 177 and 224 makes this interpretation speculative. In 1993 and 1995 (McDonald et al., 2000), the contours of HNO<sub>3</sub> greater than 1 ppbv between 25 and 35 km at day 177 closed a few days later – the contours between 27 and 37 km at day 225 had descended rapidly from the earlier enhancement at 45–50 km. Such enhancement and descent of NO<sub>y</sub> is important because it brings extra NO<sub>y</sub> to a low enough altitude that the resultant extra NO<sub>2</sub> in sunlight rapidly deactivates any chlorine above 50 hPa in late October, forming inactive ClONO<sub>2</sub>.

The enhancement has now been explained by De Zafra and Smyshlyaev (2001): production of NO<sub>y</sub> above the stratosphere in Antarctica is a maximum in midwinter (Solomon et al., 1982), provided that heterogeneous conversion of the NO<sub>2</sub> to HNO<sub>3</sub> can occur well above the altitudes of polar stratospheric clouds; mechanisms for such conversion have now been explored by various authors; and there are sufficient ion clusters and sulphate aerosol at these altitudes for the reactions to proceed (De Zafra and Smyshlyaev, 2001). In a detailed calculation, De Zafra and Smyshlyaev (2001) reproduce the mean HNO<sub>3</sub> observed in the three winters with good accuracy. The recurrent behaviour in the three winters of HNO<sub>3</sub> measurements from South Pole suggest that heterogeneous conversion may well be the norm. Further monitoring of HNO<sub>3</sub> from South Pole, planned to continue for several years, will resolve the issue.

POAM measurements of NO<sub>2</sub> in late winter in Antarctica show some similar enhancements and descent, but with large differences from year-to-year (Randall et al., 1998, 2001). The NO<sub>2</sub> enhancements have some correlation with the auroral activity index Ap (Siskind et al., 2000). During the three winters of HNO<sub>3</sub> measurements, the Ap index was between the minimum and maximum values of the 1990s (Siskind et al., 2000; Randall et al., 2002) so that the similar behaviour of HNO<sub>3</sub> enhancements in each year could be fortuitous. However, the major heterogeneous conversion of NO<sub>2</sub> to HNO<sub>3</sub> calculated by De Zafra and Smyshlyaev (2001) suggests that some of the variability observed by POAM in NO<sub>2</sub> profiles could be due to variability in the degree of conversion to HNO<sub>3</sub> during the descent process, possibly because of the temperature dependence of the conversion rate.

### 3.7. UV dose in southern South America

A commonly used diagnostic of the potential for UV to damage people is the erythemally weighted

irradiance. This can be derived from high-quality measurements of spectral irradiance by multiplying by the erythemal action spectrum. Fig. 8 shows the daily maxima of irradiances at Ushuaia during the APE-GAIA campaign period, as well as daily maxima earlier in the 1990s from this important monitoring site.

Fig. 8 also includes calculated UV using the mean ozone in the late 1970s and early 1980s, before the ozone hole was well developed. It is clear by eye that in the 1990s, measured values exceeded calculated values more often than not, and that by 1999 over 75% of the measured values were larger than calculated. The figure highlights why ozone loss is very important to southern South America: measured UV is now sometimes twice what one would expect, with a correspondingly increased potential for UV damage to people. Even in early October (spring), erythemally weighted UV can exceed  $18 \mu\text{W cm}^{-2}$ . This is comparable to the  $21 \mu\text{W cm}^{-2}$  observed in summer at Athens (Mantis et al., 2000), at the latitude of Mediterranean seaside resorts well known for giving severe sunburn to unwary fair-skinned people.

Further monitoring of UV will continue at Ushuaia, in order to establish statistically significant trends there. The necessary duration of the measurements at Ushuaia is longer than at other sites, because the large and variable amounts of cloud there cause major variability in UV.

## 4. Conclusions

A comprehensive suite of ground-based stratospheric remote sounders is now deployed in Antarctic regions and many radiosondes and ozonesondes are regularly launched. Many of their measurements, plus some additional measurement series, supported the APE-GAIA campaign in September and October 1999 in real time, to help decisions about flight plans. Their measurements will also give extensive support to scientific conclusions from the airborne measurements. However, their measurements are also allowing important scientific studies in their own right, often aided by being part of long-term monitoring activities.

Many of these studies will respond to contradictions exposed by the measurements:

- (a) The value of total NO<sub>2</sub> in midwinter appears to differ between nearby sites, but may possibly be due to differences in analysis procedures.
- (b) There is widespread layering in ozone profiles, but at least one back trajectory from an ozone maximum does not originate nearer the vortex edge.

- (c) The wave and PSC event over the Antarctic Peninsula during the flight of 2 October may be a mixture of Rossby and lee waves and so not localized, but the climatology of such mixed events is unknown.
- (d) The mean amplitude of internal gravity waves over the Antarctic Peninsula may be smaller than that of other recent studies, and the frequency of lee waves may be smaller than previously supposed. The few balloon flights analysed so far cannot give definitive results, but there may be enough flights from long-term monitoring activities at the sites to allow a resolution.  
Other studies are helping to complete some long-standing investigations:
- (e) Launches of radiosondes at two extra sites on the Antarctic Peninsula will allow us to examine the effect of meteorological analyses with and without radiosonde data on diagnoses of large mixing in the lowermost stratosphere in the Antarctic spring.
- (f) A third year of midwinter enhancement of upper stratospheric HNO<sub>3</sub> has stimulated a model study which shows it to be consistent with chemistry on ion clusters and on sulphate aerosol.
- (g) Further monitoring of UV dose in southern South America will be necessary to demonstrate the significance of ozone loss in this important area, where the edge region of the ozone hole passes over populated areas when the Sun is high enough in the sky for major UV damage.

## Acknowledgement

We thank J. Araujo and R. Sanchez (DNA, Argentina) for assistance with data collection at Belgrano; Javier Correa, Mario J. Garcia, Ricardo Sanchez, Omar Skrivanelli and Miguel Palacios for operational help at Marambio; and George Fell and Mark Jeffrey for balloon launches at Rothera. We thank the Programma Nazionale di Ricerche in Antartide (PNRA-Italy) for its support of the APE-GAIA campaign. Work at BAS was partly supported by NERC Grant GST-03/2407 from the UTLS-Ozone programme.

## References

- Arlander, W., et al. (15 authors), Quantification and interpretation of long-term UV-visible observations of the stratosphere (QUILT), proposal to EU 5th Framework Programme for project EVK2-2000-00545, 1999.
- Bacmeister, J.T., Schoeberl, M.R., Lait, L.R., Newman, P.A. ER-2 mountain wave encounter over Antarctica: evidence for blocking. *Geophys. Res. Lett.* 17, 81–84, 1990.
- Cairo, F., et al. (11 authors), A large event of polar stratospheric cloud observed over the Antarctic Peninsula with the airborne laser backscatterometer MAS and lidar MAL in comparison with synoptic and mesoscale modelling, in: Sapporo, R.D., Bojkov & Shibasaki (Eds.), *Proc. of the XIX Quad. Ozone Symp.*, NASDA, Hokaido, Japan, pp. 327–328, 2000.
- Carli, B., Cortesi, U., Redaelli, G., Blom, C., Chipperfield, M.P. The APE-GAIA campaign (Airborne Polar Experiment, Geophysica Aircraft in Antarctica). *SPARC Newsletter (Stratospheric Processes and their Role in Climate)* 15, 21–24, 2000.
- Carlsaw, K.S., et al. (10 authors), Particle microphysics and chemistry in remotely observed mountain polar stratospheric clouds. *J. Geophys. Res.* 103, 5758–5796, 1998.
- De Zafra, R.L., Smyshlyaev, S.P. On the formation of HNO<sub>3</sub> in the Antarctic mid-to-upper stratosphere in winter. *J. Geophys. Res.* 106, 23,115–23,125, 2001.
- De Zafra, R.L., Chan, V., Crewell, S., Trimble, C., Reeves, J.M. Millimeter wave measurements over the South 3. The behavior of stratospheric nitric acid through the polar fall, winter, and spring. *J. Geophys. Res.* 102, 1399–1410, 1997.
- Farman, J.C., Gardiner, B.G., Shanklin, J.D. Large losses of total ozone in Antarctica reveal seasonal ClO<sub>x</sub>/NO<sub>x</sub> interaction. *Nature* 315, 207–210, 1985.
- Ferretti, R., Paolucci, T., Bernardini, L., Redaelli, G., Dragani, R., Visconti, G. A model forecasted lee-wave event during the APE GAIA airborne experiment, in: *Proc. of the X NCAR Mesoscale Model Users Workshop*, Boulder (USA), pp. 103–106, 2000.
- Gil, M., Cacho, J. NO<sub>2</sub> total column evolution during the 1989 spring at Antarctic Peninsula. *J. Atmos. Chem.* 15, 187–200, 1992.
- Lee, A.M., Jones, R.L., Kilbane-Dawe, I., Pyle, J.A. Diagnosing ozone loss in the extratropical lower stratosphere. *J. Geophys. Res.* 107, doi: 10.1029/2001JD000538, 2002.
- Lee, A.M., Roscoe, H.K., Jones, A.E., Haynes, P.H., Shuckburgh, E.F., Morrey, M.J., Pumphrey, H.C. The impact of the mixing properties within the Antarctic stratospheric vortex on ozone loss in spring. *J. Geophys. Res.* 106, 3203–3212, 2001.
- Mantis, H.T., Repapis, C.C., Philandras, C.M., Paliatsos, A.G., Zerefos, C.S., Bais, A.F., Meleti, C., Balis, D.S. A 5-year climatology of the solar erythemal ultraviolet in Athens, Greece. *Int. J. Climatol.* 20, 1237–1247, 2000.
- McDonald, M., de Zafra, R.L., Muscari, G. Millimeter wave measurements over the South Pole, 5. Morphology and evolution of HNO<sub>3</sub> vertical distribution, 1993 versus 1995. *J. Geophys. Res.* 105, 17,739–17,750, 2000.
- Randall, C.E., Rusch, D.W., Bevilacqua, R.M., Hoppel, K.W., Lumpe, J.W. Polar ozone and aerosol measurement (POAM) II stratospheric NO<sub>2</sub>, 1993–1996. *J. Geophys. Res.* 103, 28,361–28,371, 1998.
- Randall, C.E., Siskind, D.E., Bevilacqua, R.M. Stratospheric NO<sub>x</sub> enhancements in the southern hemisphere polar vortex in winter and spring of 2000. *Geophys. Res. Lett.* 28, 2385–2388, 2001.
- Roscoe, H.K., Lee, A.M. Increased stratospheric greenhouse gases could delay recovery of the ozone hole and of ozone loss at southern mid-latitudes. *Adv. Space Res.* 28, 965–970, 2001.
- Roscoe, H.K., Charlton, A.J., Fish, D.J., Hill, J.G.T. Improvements to the accuracy of measurements of NO<sub>2</sub> by zenith-sky visible spectrometers II: errors in offset using a more complete chemical model. *J. Quantum Spectrosc. Radiat. Trans.* 68, 337–349, 2000.
- Roscoe, H.K., et al. (42 authors) Slant column measurements of O<sub>3</sub> and NO<sub>2</sub> during the NDSC intercomparison of zenith-sky UV-visible spectrometers in June 1996. *J. Atmos. Chem.* 32, 281–314, 1999.
- Shindell, D.T., Rind, D., Lonergan, P. Increased polar stratospheric ozone losses and delayed eventual recovery owing to increased greenhouse-gas concentrations. *Nature* 392, 589–592, 1998.

- Siskind, D.E., Nedoluha, G.E., Randall, C.E., Fromm, M., Russell III, J.M. An assessment of southern hemisphere stratospheric NO<sub>x</sub> enhancements due to transport from the upper atmosphere. *Geophys. Res. Lett.* 27, 329–332, 2000.
- Solomon, S., Crutzen, P.J., Roble, R.G. Photochemical coupling between the thermosphere and the lower atmosphere. *J. Geophys. Res.* 87, 7206–7220, 1982.
- Whiteway, J.A. Enhanced and inhibited gravity wave spectra. *J. Atmos. Sci.* 56, 1344–1352, 1999.
- Wirth, M., et al. (9 authors) Model-guided Lagrangian observation and simulation of mountain polar stratospheric clouds, *J. Geophys. Res.* 104, 23,971–23,981, 1999.
- Yoshiki, M., Sato, K. A statistical study of gravity waves in the polar regions based on operational radiosonde data. *J. Geophys. Res.* 105, 17,995–18,011, 2000.